An Analytic Method for Calculating the Magnetic Field Due to a Deflection Yoke

Basab B. Dasgupta
RCA Consumer Electronics, 600 N. Sherman Drive,
Indianapolis, IN 46201

Abstract—An analytical method is developed for calculating the magnetic field produced by a magnetic deflection yoke. The method can be applied to get quantitatively correct results for an air-cored saddle coil or a toroidal coil wound on a magnetic core and qualitative results for a saddle coil in the presence of a core. The final result appears in the form of angular Fourier expansions of the field components about the yoke axis where each Fourier component is expressed as a simple one-dimensional integral of known functions. As an example of application of our formalism, the magnetic field functions $H_0(z)$ and $H_2(z)$ are calculated for a specific yoke and compared with their values computed by a completely numerical scheme. The agreement between the two sets of values is very satisfactory.

1. Introduction

Calculation of the magnetic field produced by a magnetic deflection yoke used in color televisions is a formidable problem, mainly because of the peculiar geometry of the yoke. All analytical calculations that can be found in the literature[1-6] have been confined to treating the fields at points on or near the yoke axis and/or restricted to yokes of very simple unrealistic geometries. Recently, a number of very sophisticated computer programs have been developed that compute the field numerically at any point inside the television tube.[7-9] These programs, although very accurate, are expensive to run and do not shed much light on the physical aspect of the problem. In this paper we report an analytical and accurate

method for calculating the magnetic field at an arbitrary point in space due to a saddle-shaped pair of coils *without* a magnetic core. The result appears in the form of Fourier expansions of each component of the magnetic field in a polar angle about the z-axis, and each Fourier component is in the form of an integral of a closed-form expression over z, the z axis being the yoke axis. With some modifications the result can be qualitatively applied to a saddle-wound coil and quantitatively applied to a toroidal coil in the presence of a magnetic core. This result would be very useful in understanding the dependence of the various field components on location of the field point, the geometry of the coil and its wire distribution. It would also save computer time in computing various quantities of interest to yoke designers that depend on the magnetic field components.

The paper is organized as follows. The calculation of magnetic field due to a saddle-shaped coil is divided into two parts: (a) calculation of field due to the main body of the yoke, which is assumed to be a current sheet with a certain surface current density distribution (determined by the actual angular distribution of the wires in the coil), and (b) calculation of field due to the end-turns, which are assumed to be circular arcs with a certain prescribed distribution along the z-direction. The first part is presented in Sec. 2 and the second part in Sec. 3. In Sec. 4 we discuss the modifications necessary to make our results applicable to a coil in the presence of a magnetic core. Sec. 5 is devoted to a numerical calculation of the magnetic field functions $H_0(z)$ and $H_2(z)$, which are of interest in the third-order aberration theory,[2,3] for a yoke under development at RCA on the basis of our theory. The same two functions are also calculated using an elaborate computer technique by following the methods described in Ref. [8], and the results are compared with our results. The agreement is very satisfactory. We conclude in Sec. 6 by suggesting some possible applications of our results.

2. Field Due to a Current Sheet of Revolution

We will use a cylindrical coordinate system (ρ, θ, z) in our derivation. We will assume the main deflecting part of the yoke to be a current sheet symmetric about the z-axis with a profile described by the function $\rho_0(z)$ (see Fig. 1). This profile is very similar to the profile of the neck of the cathode-ray tube and is usually expressed by a polynomial in z. The surface current density on the sheet $K(\rho_0, \theta, z)\mathbf{a}_K$ has a magnitude which can be expressed as a Fourier series

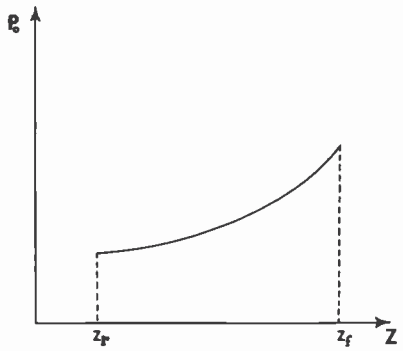

Fig. 1—The profile of the current sheet representing a saddle coil in the ρ-*z* plane.

$$K(\rho_0, \theta, z) \equiv \frac{I\lambda(\theta, z)}{\rho_0(z)} = \frac{I}{\rho_0(z)_{m=1,3,5\ldots}} \sum f_m(z) \cos m\theta. \quad [1]$$

Here I is the current in each turn of the coil and $\lambda d\theta$ is the number of turns passing between the angles θ and $\theta + d\theta$ at a cross-section located at z. In writing Eq. [1] it is assumed that the x-axis lies along the horizontal direction if the coil is supposed to produce horizontal deflection and along the vertical direction if the coil is supposed to produce vertical deflection. The direction of the current density expressed by the unit vector $\boldsymbol{a}_K$ is *assumed* to be given by

$$\boldsymbol{a}_K = (\cos\theta\ \rho_0'\ \boldsymbol{a}_x + \sin\theta\ \rho_0'\ \boldsymbol{a}_y + \boldsymbol{a}_z)/(1 + \rho_0'^2)^{1/2}, \quad [2]$$

where $\boldsymbol{a}_x$, $\boldsymbol{a}_y$, $\boldsymbol{a}_z$ are unit vectors along x, y, z, axes and a prime indicates derivative with respect to z. Physically this means that the current flows along the profile of the coil-sheet in the (ρ, z) plane and along the radial lines in the (x, y) planes. Note, however, that this assumption does *not* imply that there is no bias in the coil, because λ in Eq. [1] is allowed to be z-dependent.

The magnetic field at an arbitrary point (ρ, θ, z) due to this current sheet can be obtained by applying the Biot-Savart law[10]

$$\boldsymbol{H}(\rho, \theta, z) = \int \frac{\boldsymbol{K}(\rho_0, \theta_0, z_0) \times \boldsymbol{R}\ ds}{4\pi R^3} \quad [3]$$

where ds is an element of surface area located at (ρ_0, θ_0, z_0) on the sheet and given by

$$ds = \rho_0(1 + \rho_0'(z_0)^2)^{1/2} d\theta_0 dz_0 \quad [4]$$

$$\boldsymbol{R} = (\rho\cos\theta - \rho_0\cos\theta_0)\boldsymbol{a}_x + (\rho\sin\theta - \rho_0\sin\theta_0)\boldsymbol{a}_y + (z - z_0)\boldsymbol{a}_z \quad [5]$$

$$R = \{\rho^2 + \rho_0^2 - 2\rho\rho_0\cos(\theta - \theta_0) + (z - z_0)^2\}^{1/2} \quad [6]$$

and the integration in Eq. [3] extends over the entire surface area of the sheet. After some straight-forward algebra it can be shown that the cylindrical components of $\boldsymbol{H}$ are given by

$$H_\rho(\rho, \theta, z) = \frac{1}{4\pi} \int dz_0 \int_0^{2\pi} d\theta_0 \, K(\rho_0, \theta_0, z_0) \frac{\rho_0 \sin(\theta_0 - \theta)}{R^3} [\rho_0'(z_0)(z - z_0) + \rho_0(z_0)], \quad [7]$$

$$H_\theta(\rho, \theta, z) = \frac{1}{4\pi} \int dz_0 \int_0^{2\pi} d\theta_0 \, K(\rho_0, \theta_0, z_0) \frac{\rho_0}{R^3} \times [-\cos(\theta_0 - \theta) \{\rho_0'(z_0)(z - z_0) + \rho_0(z_0)\} + \rho_0(z_0)], \quad [8]$$

$$H_z(\rho, \theta, z) = \frac{1}{4\pi} \int dz_0 \int_0^{2\pi} d\theta_0 \, K(\rho_0, \theta_0, z_0) \frac{\rho_0}{R^3} \rho_0'(z_0) \sin(\theta - \theta_0). \quad [9]$$

The z_0 integrals in Eqs. [7]–[9] extend from the rear-end to the front-end of the yoke.

Using the symmetry of the coil the magnetic field components can be expanded in the following way:

$$H_\rho(\rho, \theta, z) = \sum_n H_\rho^n(\rho, z) \sin n\theta \quad [10]$$

$$H_\theta(\rho, \theta, z) = \sum_n H_\theta^n(\rho, z) \cos n\theta \quad [11]$$

$$H_z(\rho, \theta, z) = \sum_n H_z^n(\rho, z) \sin n\theta. \quad [12]$$

The summations in Eqs. [10]–[12] and all sums over indices m and n in our subsequent discussion are implied to run over the odd positive integers. The nth harmonic component of H_ρ can be calculated using the usual Fourier formula

$$H_\rho^n(\rho, z) = \frac{1}{\pi} \int_0^{2\pi} H_\rho(\rho, \theta, z) \sin n\theta d\theta. \quad [13]$$

Substituting Eqs. [1] and [7] into Eq. [13] and changing the variable $(\theta_0 - \theta)$ to α we get

$$H_\rho^n(\rho, z) = \sum_m \frac{I}{4\pi^2} \int_0^{2\pi} d\theta \sin n\theta \int dz_0 f_m(z_0)[\rho_0'(z_0)(z - z_0) + \rho_0]$$

$$\times \int_{-\theta}^{2\pi-\theta} d\alpha \frac{\cos m(\alpha + \theta)\sin\alpha}{[\rho^2 + \rho_0^2 - 2\rho\rho_0\cos\alpha + (z - z_0)^2]^{3/2}} \quad [14]$$

If we now write

$$\cos m(\alpha + \theta)\sin n\theta = {}^1/_2[\sin\{(n + m)\theta + m\alpha\} - \sin\{(n - m)\theta - m\alpha\}] \quad [15]$$

and integrate partially with respect to θ, it is easy to show that only the term with $m = n$ survives in the summation appearing in Eq. [14] and gives

$$H_\rho^n(\rho, z) = -\frac{I}{4\pi} \int dz_0 f_n(z_0)[\rho_0'(z_0)(z - z_0) + \rho_0] \times \int_0^{2\pi} d\alpha \frac{\sin n\alpha \sin\alpha}{[\rho^2 + \rho_0^2 - 2\rho\rho_0\cos\alpha + (z - z_0)^2]^{3/2}}. \quad [16]$$

The integral over α can be performed by introducing the variable $\phi = \alpha/2$, expanding $\sin n\alpha$ as

$$\sin n\alpha \equiv \sin 2n\phi = \sum_{k=1}^{n} (-1)^{k+1} \binom{2n - k}{k - 1} 2^{2n-2k+1} \sin\phi \cos^{2n-2k+1}\phi \quad [17]$$

and integrating term by term.

The final result for H_ρ^n can be expressed as

$$H_\rho^n(\rho, z) = -\frac{I}{2\pi} \sum_{k=1}^{n} (-1)^{k+1} \binom{2n - k}{k - 1} 2^{2n-2k+1} B\left(\frac{3}{2}, \frac{2n - 2k + 3}{2}\right) \int dz_0 f_n(z_0)[\rho_0'(z_0)(z - z_0) + \rho_0(z_0)] \frac{1}{q^{3/2}} \times F\left(\frac{2n - 2k + 3}{2}, \frac{3}{2}; n - k + 3; \frac{4\rho\rho_0}{q}\right) \quad [18]$$

where

$$q = (\rho + \rho_0)^2 + (z - z_0)^2 \quad [19]$$

Here $F(a, b; c; x)$ is the hypergeometric function[11] and $B(x, y)$ is the beta function.[12]

Similar manipulations can be carried out to determine $H_\theta^n(\rho, z)$ and $H_z^n(\rho, z)$. For H_θ^n we get

$$H_\theta^n(\rho, z) = -\frac{I}{4\pi}\int dz_0 f_n(z_0)[\rho_0'(z_0)(z - z_0) + \rho_0(z_0)] \times \int_0^{2\pi} d\alpha \frac{\cos n\alpha \cos\alpha}{[\rho^2 + \rho_0^2 - 2\rho\rho_0\cos\alpha + (z - z_0)^2]^{3/2}} + \frac{I\rho}{4\pi}\int dz_0 f_n(z_0) \int_0^{2\pi} d\alpha \frac{\cos n\alpha}{[\rho^2 + \rho_0^2 - 2\rho\rho_0\cos\alpha + (z - z_0)^2]^{3/2}} \quad [20]$$

To do the α integrals we now need the following expansion

$$\cos n\alpha \equiv \cos 2n\phi = \sum_{k=1}^{n+1} (-1)^{k+1} \binom{2n}{2k-2} \cos^{2n-2k+2}\phi \sin^{2k-2}\phi \quad [21]$$

The final expression for H_θ^n is

$$H_\theta^n(\rho, z) = -\frac{I}{2\pi}\sum_{k=1}^{n+1} (-1)^{k+1} \binom{2n}{2k-2} B\left(\frac{2k-1}{2}, \frac{2n-2k+5}{2}\right) \times \int dz_0 f_n(z_0)[\rho_0'(z_0)(z - z_0) + \rho_0(z_0)] \frac{1}{q^{3/2}} F\left(\frac{2n-2k+5}{2}, \frac{3}{2}; n+3; \frac{4\rho\rho_0}{q}\right) + \frac{I}{4\pi}\sum_{k=1}^{n+1} (-1)^{k+1} \binom{2n}{2k-2} B\left(\frac{2k-1}{2}, \frac{2n-2k+3}{2}\right) \times \int dz_0 f_n(z_0)[\rho'(z_0)(z - z_0) + \rho_0(z_0) + \rho]\frac{1}{q^{3/2}} F\left(\frac{2n-2k+3}{2}, \frac{3}{2}; n+1; \frac{4\rho\rho_0}{q}\right). \quad [22]$$

Similarly, H_z^n can be written in the final form as

$$H_z^n(\rho, z) = \frac{\rho I}{4\pi}\sum_{k=1}^{n} (-1)^{k+1} \binom{2n-k}{k-1} 2^{2n-2k+1} B(1, n-k+1) \int dz_0 f_n(z_0)\rho_0'(z_0) \frac{1}{q^{3/2}} F\left(n-k+1, \frac{3}{2}; n-k+2; \frac{4\rho\rho_0}{q}\right). \quad [23]$$

Eqs. [18], [22], and [23] constitute the desired analytical expressions for the magnetic field due to the current sheet.

As a special case we note from Eqs. [16] and [20] that H_ρ^n and H_θ^n are zero on the yoke axis ($\rho = 0$) for all $n \neq 1$ and $H_z^n = 0$ at $\rho = 0$ for all n. The axial magnetic field $H_0(z)$ is equivalent to $H_\rho^1(\rho = 0, z)$ and is given from Eq. [18] by

$$H_0(z) = -\frac{I}{4} \int dz_0 f_1(z) \frac{[\rho_0'(z_0)(z - z_0) + \rho_0(z_0)]}{[\rho_0^2 + (z - z_0)^2]^{3/2}}. \quad [24]$$

3. Field Due to the End Turns

Let us first assume that both the front and rear end-turns can be approximated by certain single effective circular arcs about the z axis with certain mean radii and mean lengths but zero thicknesses. Fig. 2 shows the "effective" front end-turn defined in this way; the top half starts and ends at angles θ_f and $\pi - \theta_f$, respectively, has a radius a, and carries the current in the counter clockwise direction while the bottom half is just its "mirror image" about the x axis. If z_f is the location of the front end-turns and there are N turns in each half of the coil, the magnetic field dH at (ρ, θ, z) due to an element of length dL of this effective end-turn is again given by the Biot-Savart law:

$$dH = \frac{NI(dL \times R)}{4\pi R^3}, \quad [25]$$

where

$$dL = \pm a d\theta_0 \mathbf{a}_\theta. \quad [26]$$

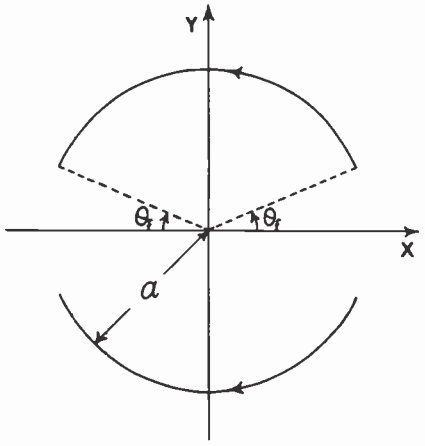

Fig. 2—The "effective" circular front end-turn of a saddle coil.

The upper and lower signs apply to the upper and lower halves of the turn, respectively, and R, R are given by Eqs. [5] and [6] respectively with ρ_0 replaced by a and z_0 replaced by z_f. To get the total field one has to integrate the expression [25] over θ_0 from θ_f to $\pi-\theta_f$ to take into account the upper half of the turn and then from $\pi + \theta_f$ to $2\pi-\theta_f$ to include the contribution of the lower half. After some simple algebra, the components of the field can be easily shown to be

$$H_\rho(\rho, \theta, z) = \frac{NIa(z - z_f)}{4\pi}\int_{\theta_f}^{\pi-\theta_f} \cos(\theta - \theta_0)\left[\frac{1}{R_-^3} + \frac{1}{R_+^3}\right]d\theta_0 \qquad [27]$$

$$H_\theta(\rho, \theta, z) = \frac{NIa(z - z_f)}{4\pi}\int_{\theta_f}^{\pi-\theta_f} \sin(\theta_0 - \theta)\left[\frac{1}{R_-^3} + \frac{1}{R_+^3}\right]d\theta_0 \qquad [28]$$

$$H_z(\rho, \theta, z) = \frac{NIa}{4\pi}\int_{\theta_f}^{\pi-\theta_f}\left[\frac{a - \rho\cos(\theta - \theta_0)}{R_-^3} - \frac{a + \rho\cos(\theta - \theta_0)}{R_+^3}\right]d\theta_0 \qquad [29]$$

where

$$R\pm = [\rho^2 + a^2 \pm 2\rho a\cos(\theta - \theta_0) + (z - z_f)^2]^{1/2}. \qquad [30]$$

All the integrals appearing in Eqs. [27]–[29] can be evaluated in closed-forms, but since we expressed the magnetic field due to the main body of the coil as Fourier series in θ we will do the same thing here and give explicit expressions for the Fourier coefficients. Thus using Eqs. [10] and [27], integrating by parts with respect to θ and after some manipulations, we get

$$H_\rho^n(\rho, z) = \frac{NIa(z - z_f)}{\pi n}\cos n\,\theta_f\int_0^\pi \frac{\cos n\alpha\,\cos\alpha\,d\alpha}{\{\rho^2 + a^2 - 2\rho a\cos\alpha + (z - z_f)^2\}^{3/2}}$$

or

$$H_\rho^n(\rho, z) = \frac{NIa(z - z_f)}{\pi n}\cos n\theta_f\sum_{k=1}^{n+1}(-1)^{k+1}\binom{2n}{2k-2}\frac{1}{q_f^{3/2}}$$
$$\times\left[2B\left(\frac{2k-1}{2}, \frac{2n-2k+5}{2}\right)F\left(\frac{2n-2k+5}{2}, \frac{3}{2}; n+3; \frac{4a\rho}{q_f}\right)\right.$$
$$\left. - B\left(\frac{2k-1}{2}, \frac{2n-2k+3}{2}\right)F\left(\frac{2n-2k+3}{2}, \frac{3}{2}; n+1; \frac{4a\rho}{q_f}\right)\right] \qquad [31]$$

where

$$q_f = (\rho + a)^2 + (z - z_f)^2 \qquad [32]$$

Similarly, using Eqs. [11], [12], [28], and [29] we get

$$H_\theta^n(\rho, z) = -\frac{NIa(z - z_f)}{\pi n}\cos n\theta_f \sum_{k=1}^{n} (-1)^{k+1}\binom{2n-k}{k-1} 2^{2n-2k+1} \times \frac{1}{q_f^{3/2}} B\left(\frac{3}{2}, \frac{2n-2k+3}{2}\right) F\left(\frac{2n-2k+3}{2}, \frac{3}{2}, n-k+3; \frac{4a\rho}{q_f}\right) \qquad [33]$$

and

$$H_z^n(\rho, z) = -\frac{\rho}{(z - z_f)} H_\rho^n(\rho, z) - \frac{NIa^2}{\pi n}\cos n\theta_f \sum_{k=1}^{n+1} (-1)^{k+1}\binom{2n}{2k-2} \times \frac{1}{q_f^{3/2}} B\left(\frac{2k-1}{2}, \frac{2n-2k+3}{2}\right) F\left(\frac{2n-2k+3}{2}, \frac{3}{2}; n+1; \frac{4a\rho}{q_f}\right). \qquad [34]$$

Again in the special case of $\rho = 0$, Eq. [31] reduces to

$$H_\rho^1(0, z) \equiv H_0(z) = -\frac{NIa(z - z_f)\cos\theta_f}{2[a^2 + (z - z_f)^2]^{3/2}}, \qquad [35]$$

which agrees with the result given in Ref. [2].

Similarly if the rear end-turns are approximated by mean circular arcs of radii b, starting angle θ_r located at $z = z_r$, the Fourier coefficients of the magnetic field produced by them can be obtained from Eqs. [31], [33], and [34] by replacing a by b, the subscript f by r and changing the over-all signs to take into account the opposite direction of current.

Several generalizations of Eqs. [31], [33], and [34] are possible. First of all, we note that not all end-turns start at one angle. If we look at the front end-turns, for example, there are $\lambda(\theta_f, z_f)d\theta_f$ number of turns which start between the angles θ_f and $\theta_f + d\theta_f$, where the function λ is given by Eq. [1], i.e.,

$$\lambda(\theta_f, z_f) = \sum_m f_m(z_f)\cos m\theta_f. \qquad [36]$$

We can easily take into account this angular distribution of turns by writing $\lambda(\theta_f, z_f)d\theta_f$ for N in Eqs. [31], [33], and [34] and inte-

grating over θ_f from 0 to $\pi/2$. If the radius a of the turns were independent of θ_f the net result of this integration would have been replacing the quantity $N\cos n\theta_f$ in these expressions by $\pi f_n(z_f)/4$; but since a depends on θ_f each Fourier component of the magnetic field would involve all wire distribution harmonics $f_m(z_f)$. It is also true in reality that the end-turns do not lie in a single plane but have a certain thickness in the z-direction. This can be included in our theory by replacing $f_m(z_f)$ in Eq. [36] by some distribution of turns along z, $f_m(z_f)dz_f$ say, and integrating the resultant expressions for the field components over z_f. Again one has to keep in mind that the radius a would also be a function of z_f. The main difficulty in a practical computation is that the dependence of a on θ_f and z_f and the distribution of end-turns, $f_m(z_f)$, over their thickness are not very precisely known because they remain to a large extent at the mercy of the winding machine. If these functional relations can somehow be determined, the integrations over θ_f and/or z_f can be done numerically using a simple computer program. A similar comment applies to the rear end-turns as well. Another complexity of the end-turns, especially at the rear end, is that even though the turns might be circular arcs their centers may not lie on the z-axis. One can include this "off-centering" in the present treatment by an appropriate coordinate transformation. Finally, we want to point out that we need not restrict ourselves to circular end-turns; other unconventional shapes of end-turns such as rectangular and hexagonal[13] can also be taken into account in the present theory in a straightforward way.

4. Effect of the Core

The theoretical treatment given so far is valid if there is no magnetic core present in the yoke. When a core is present, it changes the magnetic field substantially. The relative permeability of the typical core material used in commercial yokes is quite high, of the order of 1000, and can be assumed to be infinity for all practical purposes. It can be shown[14] that for a long cylindrical yoke, the effect of such a high-permeability core is to multiply the n-th Fourier component of the magnetic field by the factor $[1 + (\rho_0/\rho_c)^{2n}]$, where ρ_0 and ρ_c are the coil and core radii, respectively; this result can be derived by solving the Laplace's equation for the z-component of the vector potential,

$$\nabla^2 A_z = 0 \qquad [37]$$

in the (ρ, θ) plane and using the usual boundary conditions at $\rho =$

ρ_0 and $\rho = \rho_c$. In view of this result, we can take into account the effect of the core in a qualitative way by introducing the following major simplication in our theory. We assume that the effect of a core on the magnetic field *inside* the yoke produced by the main body of the coil can be simulated by replacing the harmonic components $f_n(z)$ of the turn distribution by the functions

$$\tilde{f}_n(z) = [1 + \{\rho_0(z)/\rho_c(z)\}^{2n}]f_n(z) \qquad [38]$$

in Eqs. [18], [22], and [23]. Physically this means that each cross-section of the yoke is assumed to behave, as far as the effect of the core on the magnetic field is concerned, as if it were part of an infinitely long cylindrical yoke with that cross-section.

In the case of a toroid-shaped coil wound on the core, $\rho_0(z) = \rho_c(z)$ and Eq. [36] reduces to

$$\tilde{f}(z) = 2f_n(z). \qquad [39]$$

This result can be interpreted in terms of an "image" effect.[14] The image theorem states that if a *plane* surface of a magnetic material of infinite permeability is present in the vicinity of a current-carrying wire then the effect of the material on the magnetic field is the same as the one produced by a fictitious wire that is identical to the real wire but located on the other side of the plane surface at a distance equal to the distance of the wire from the surface. For a curved core surface the validity of this theorem, of course, becomes questionable, but if the actual coil sits right on the inner core surface, which is the case in a toroidal coil, the "image coil" coincides with the real coil both in strength and location regardless of the shape of the core surface. The magnetic field inside the yoke should then double compared to the core-free value. Eq. [39] is precisely equivalent to this statement. For a saddle coil, Eq. [38] can also be interpreted in terms of a contribution from an image coil, but in this case each harmonic component requires a different image.

It is more difficult to take into account the effect of the core on the magnetic field produced by the end-turns. The simplest approximation one can make is to assume that the contribution of the end-turns to the magnetic field is not affected by the presence of the core. At first glance this may seem like an unrealistic assumption, since a cylindrical core is known to have "shielding" effects on an external magnetic field. However, if we note that a core is typically only one inch or so in length, whereas the electron beams are deflected over a length of ten inches or more, and the field due to the end-turns is of secondary importance anyway, neglecting the shielding effect does not appear to be an overly crude assumption.

This is especially true for higher harmonics of the end-turn field which are localized near the turns.

For a toroidal coil, the effect of the core on the field produced by the end-turns is probably more drastic because of the proximity of the (radial) end-turns to the core surface, but since in this case the contributions of the end-turns to the field are quite small to begin with (because of the relatively small length of these turns compared to those of a saddle coil), we will simply ignore the end-turns altogether in calculating the field due to a toroidal coil.

5. Numerical Calculation

The numerical results calculated for a specific yoke using the expressions given in Sections 2–4 can be displayed graphically in a number of ways. One can plot each harmonic component of the magnetic fields H_ρ, H_θ, H_z or the total field as a function of ρ at a given z or as a function of z at a given ρ or along some curve in the ρ-z plane. As a first example of such numerical calculation, we have chosen to calculate and plot the magnetic field functions $H_0(z)$ ($\equiv H_y(0, 0, z)$) and $H_2(z)$ defined by

$$H_2(z) = \frac{1}{2}\left(\frac{\partial^2 H_y}{\partial x^2}\right)_{x=0,\,y=0}. \qquad [40]$$

These functions are of considerable interest in the third-order aberation theory,[2,3,15] and a knowledge of them allows one to calculate the aberration coefficients which determine the various deflection errors within the context of this theory. Another reason for choosing these quantities is that they can be experimentally measured with relative ease.

To perform a numerical calculation, one has to know the following quantities: the function $\rho_0(z)$, which represents the profile of the inner surface of the coil in the ρ-z plane; the function $\rho_c(z)$, which is the profile of the inner surface of the core; and the Fourier coefficients $f_n(z)$ of the winding distribution of the coil for each z. The first two functions are typically in the form of polynomials or a series of polynomials that join smoothly. The remaining functions can also be expressed as polynomials in z by fitting their numerical values by a polynomial-fitting routine. All the integrals involved in Eqs. [18], [22], and [23] are then simple one-dimensional integrals which can be done on a relatively small computer using a simple integration routine.

The $H_0(z)$ function due to the main body of the yoke and due to the end-turns of a saddle coil is given by Eqs. [24] and [35], respec-

tively, provided $f_1(z_0)$ in Eq. [24] is replaced by $\tilde{f}_1(z_0)$ defined by Eq. [38]. The $H_2(z)$ function can be calculated from H_ρ^1 and H_θ^3 functions according to a formula discussed in the appendix. The results are given below:

$H_2(z)$ (due to the main body of the yoke)

$$= \frac{I}{16}\int dz_0 \tilde{f}_1(z_0)\left[\frac{3(z-z_0)\rho'(z_0)+6\rho_0(z_0)}{\{\rho_0^2+(z-z_0)^2\}^{5/2}} - \frac{15}{2}\frac{\{\rho_0^2(z-z_0)\rho'(z_0)+\rho_0^3\}}{\{\rho_0^2+(z-z_0)^2\}^{7/2}}\right]$$

$$-\frac{15I}{32}\int dz_0 \tilde{f}_3(z_0)\frac{\{\rho_0^2(z-z_0)\rho'(z_0)+\rho_0^3\}}{\{\rho_0^2+(z-z_0)^2\}^{7/2}}; \qquad [41]$$

$H_2(z)$ (due to circular end turns of a saddle coil of mean radius a located at $z = z_f$ and lying between the angles θ_f and $\pi - \theta_f$ in the upper half and between $\pi + \theta_f$ and $2\pi - \theta_f$ in the lower half)

$$= \frac{NIa}{2\pi}(z-z_f)\left[\frac{5a^2\cos^3\theta_f}{\{a^2+(z-z_f)^2\}^{7/2}} - \frac{3a\cos\theta_f}{\{a^2+(z-z_f)^2\}^{5/2}}\right]. \qquad [42]$$

In this paper we have calculated the variation of the quantities $H_0(z)$ and $H_2(z)$ with z for a yoke that is currently under development at RCA. The functions $\rho_0(z_0)$ and $\rho_c(z_0)$ have been computed using a program that determines the design of the arbor cavity used to make the horizontal coil and the design of the core. The functions $f_n(z)$ were determined by a program that Fourier analyzes the angular variation of the incremental area of the arbor cavity cross-section taking into account the fact that not the entire cavity is filled uniformly with wires during winding. The points z_f, z_r were taken in the middle of the coil thickness and the angles θ_f and θ_r were chosen to be approximately half-way between the starting and finishing angles at the front- and rear-ends, respectively. We have also calculated the $H_0(z)$ function for a toroidal coil radially wound on the core of this yoke neglecting the end-turns. Our results are shown in Figs. 3, 4, and 5.

To check the accuracy of these results we have also calculated $H_0(z)$ and $H_2(z)$ by using a very sophisticated and expensive computer program. The mathematical principles behind this program is discussed in Ref. [8]; it involves replacing the coil by an effective "magnetic charge" on the core which produces the same magnetic field everywhere inside the coil. The results of these calculations are also shown in Figs. 3, 4, and 5. The two sets of results are

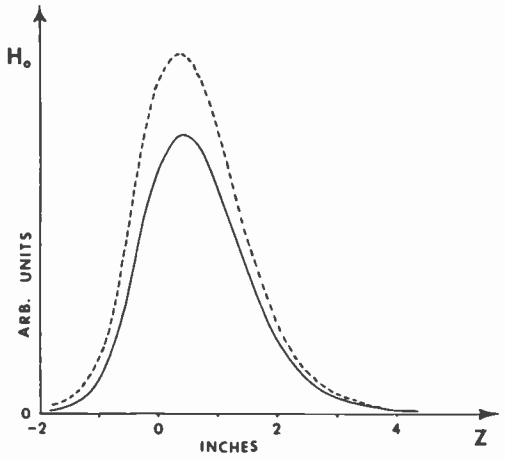

Fig. 3—The axial magnetic field $H_0(z)$ due to a nonradial saddle coil. The solid curve corresponds to the result derived in the present paper and the dashed curve corresponds to the values computed numerically by the method described Ref. [8].

strikingly similar. In particular, the general shapes of the curves and the locations of the maxima and minima are almost identical in the two cases. The two sets of curves even agree closely in absolute numbers. An exact agreement in magnitude for a saddle coil was not expected, partly because of the approximate nature of the way the core is taken into account in our theory and partly because the two theories treat the end-turns somewhat differently.

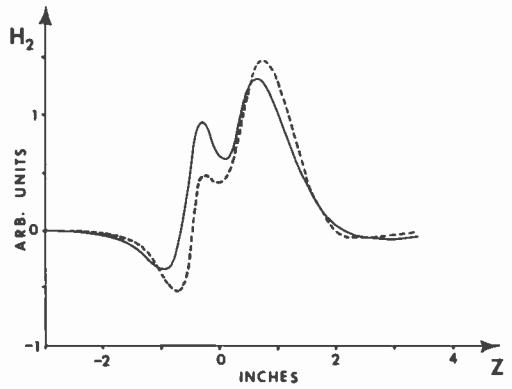

Fig. 4—The magnetic field function $H_2(z)$ due to a nonradial saddle coil. The solid curve corresponds to the result derived in the present paper and the dashed curve corresponds to the values computed numerically by the method described in Ref. [8].

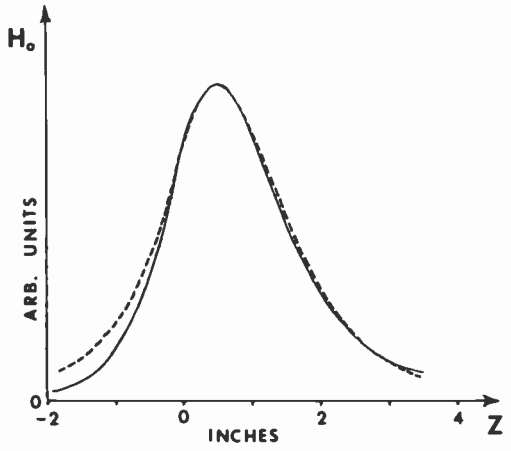

Fig. 5—The axial magnetic field $H_0(z)$ due to a radially wound toroidal coil. The solid curve corresponds to the result derived in the present paper and the dashed curve corresponds to the values computed numerically by the method described in Ref. [8].

In experiments done elsewhere[8,16] the computer-predicted variations of $H_0(z)$ and $H_2(z)$ were found to be in excellent agreement with experimental results for several yokes. Since our results agree very well with the computer calculations, this observation can also be considered as an indirect experimental verification of the present theory.

As a second example of numerical application of our theory we have calculated the various harmonic coefficients of the magnetic field components H_ρ and H_θ due to the end-turns of a saddle coil as a function of ρ using Eqs. [31] and [33] and neglecting the presence of the core. The results are shown in Figs. 6 and 7. Note that the contributions of all harmonics beyond the first are insignificant, but the first harmonic field is largely radial (i.e. pin-cushion shaped) close to the turns.

6. Concluding Remarks

We have developed an analytical method for calculating the magnetic field at an arbitrary point due to a magnetic deflection coil. The method is capable of giving quantitative results for an air-core saddle coil and qualitatively correct results in the presence of a magnetic core. The final numerical calculation of the field requires a simple numerical integration routine over one variable and a

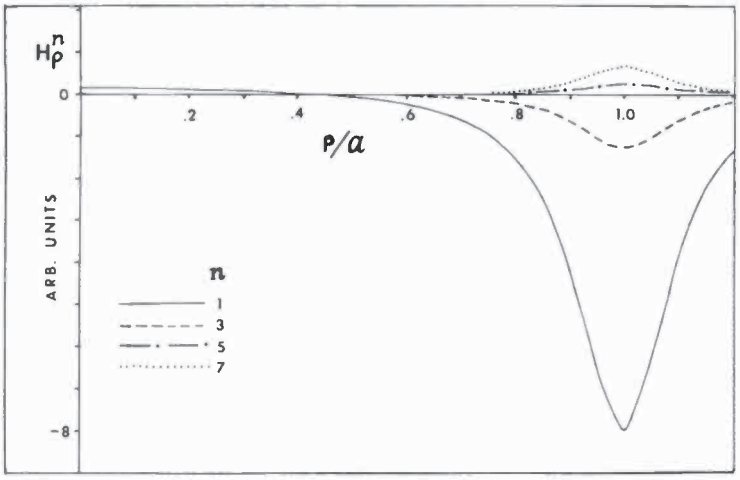

Fig. 6—The radial component of the magnetic field H_ρ as a function of ρ due to the circular end-turns of an air-core saddle coil at a distance 0.1α from the location of the end-turns. $\theta_f = 20°$.

function routine for evaluation of the hypergeometric series; both of these can be made readily available on a relatively small computer. Hence the success of the present method would imply considerable savings of computer CPU time over the numerical methods of computing the field, described in Refs. [7]–[9], and make it fea-

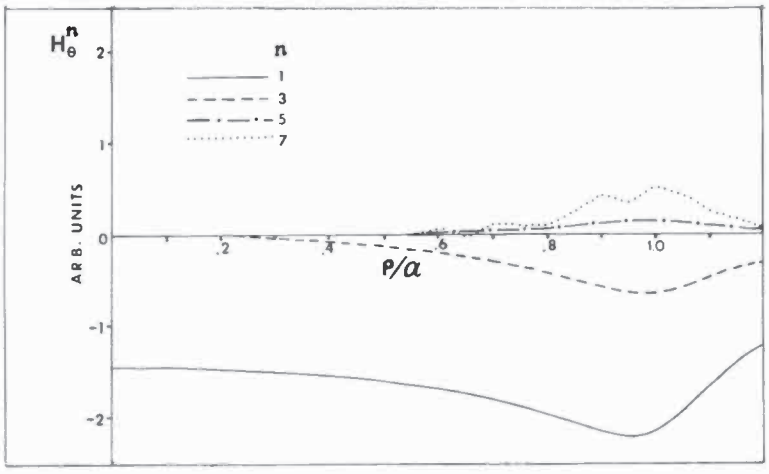

Fig. 7—The tangential component of the magnetic field H_θ as a function of ρ due to the circular end-turns of an air-core saddle coil at a distance 0.1*a* from the location of the end-turns. $\theta_f = 20°$.

sible to do these computations on a small computer. At present, for a saddle coil with a magnetic core, this success is limited because the effect of the core is not considered in a precise way, but we believe that an analytical treatment of the core could be improved, perhaps by some generalized image theorem. The present method can be easily extended to calculate the field due to the main body of a *toroidally* wound coil on a core simply by replacing $f_n(z_0)$ in Eqs. [18], [22], and [23] by $2f_n(z_0)$, the factor 2 being due to the image coil as discussed in Sec. 4. However, the core makes it difficult to calculate the field due to the end-turns of a toroidal coil.

A knowledge of the magnetic field at all points inside a television tube is extremely useful in analyzing the performance of a yoke and, in principle at least, it allows one to calculate all the characteristics relevant to its commercial use. We conclude by listing some important areas of application of our theory.

(1) Knowing the $H_0(z)$ and $H_2(z)$ functions for both coils, calculated in the previous section, one can calculate all the aberration coefficients appearing in the third-order aberration theory[2,3,15] and hence all the deflection errors produced by a yoke as predicted by this theory. Furthermore, one can determine higher-order derivatives of the field near the axis, such as the $H_4(z)$ function in the fifth-order aberration theory, from our expressions of field components.

(2) One can calculate the electron trajectories inside the tube once the magnetic field is known by solving the equations of motion of the electron. This would require a separate computer program similar to the one described in Ref. [9]. One could then determine the peak currents in both coils needed to scan the screen and other features relevant to manufacturing, such as the "pullback" distance.* The convergence errors on the screen can also be determined by first finding the coordinates of the landing points of the three primary beams and then taking the differences of various pairs of coordinates. This is not an accurate method of calculating the errors, however, since the errors are typically about 100 times smaller than the deflections of the beams and, hence, can be "washed out" by the inaccuracies in the computing method itself.

(3) Recently the author has developed a theory that relates the deflection errors directly with the harmonic components of the field.[17] The result involves integrations of expressions con-

* The pullback distance is the distance through which the yoke can be moved back starting from the tube neck before the electron beam strikes the inside glass of the tube.

taining the various field components along the trajectory of the electrons. An analytical expression for the Fourier components of the field would be extremely useful in a numerical computation of the deflection errors using this formalism.

(4) The inductance of a saddle-shaped horizontal coil can be expressed in terms of the variation of the harmonic components H_ρ^n and H_z^n along the inside coil contour.[18] Again analytical expressions for H_ρ^n and H_z^n would greatly facilitate the inductance calculation. In conjunction with the calculation of the peak horizontal current, one can then determine the so-called "stored energy" of the coil which is an important performance characteristic of a yoke.

(5) Since the present theory gives separate expressions for the field due to the main body of the yoke and the field due to the end-turns, one can study the effect of the end-turns on the various deflection errors and hence use the geometry of the end-turns as a useful parameter in the design of a yoke.

(6) Finally, one can investigate the radial variation of the various harmonic components across any given cross-section of the coil. This would tell us how the different harmonics increase in strength as the coil is approached. This knowledge is useful in understanding the importance of the various harmonics in determining the yoke performance.

Appendix

The relationship between $H_2(z)$ defined in Sec. 4 and the Fourier components of the field is best obtained by writing H_y near the yoke axis in two ways. A Taylor expansion in Cartesian coordinates yields.

$$H_y = H_0(z) - [H_2(z) + {}^1/_2 H_0''(z)]\, y^2 + H_2(z)x^2 + \ldots \qquad \text{[A-1]}$$

On the other hand H_y can be related to the magnetostatic potential harmonics in the following way.[16] The potential $\psi(\rho, \theta, z)$ has a Fourier expansion given by

$$\psi(\rho, \theta, z) = \phi_1(\rho, z)\sin\theta + \phi_3(\rho, z)\sin 3\theta + \ldots \qquad \text{[A-2]}$$

Near the axis,

$$\phi_1(\rho, z) \cong a_1(z)\rho - a_1''(z)\rho^3/8 \qquad \text{[A-3]}$$

$$\phi_3(\rho, z) \cong a_3(z)\rho^3, \qquad \text{[A-4]}$$

so that

$$H_y \equiv \frac{\partial \psi}{\partial y} = -a_1(z) + (x^2 + 3y^2)a_1''(z)/8 - 3(x^2 - y^2)a_3(z). \quad [A\text{-}5]$$

Comparing Eqs. [A-1] and [A-5], we get

$$H_0(z) = -a_1(z) \quad [A\text{-}6]$$

$$H_2(z) = +\frac{a_1''(z)}{8} - 3a_3(z). \quad [A\text{-}7]$$

Since

$$H_\rho^1(0, z) = H_0(z) = -a_1(z) \quad [A\text{-}8]$$

$$\text{and } H_3^\theta(\rho, z) = -\frac{3}{\rho}\phi_3(\rho, z), \quad [A\text{-}9]$$

we can write Eq. [A-6] as

$$H_2(z) = -\frac{H'\rho''(0, z)}{8} + \left\{\frac{1}{\rho^2} H_3^\theta(\rho, z)\right\}_{\rho = 0}. \quad [A\text{-}10]$$

This formula has been used in the paper to calculate $H_2(z)$.

References:

[1] R. G. E. Hutter, "Electron Beam Deflection—Part II. Applications of the Small-Angle Deflection Theory," *J. Appl. Phys.*, **18**, p. 797 (1947).
[2] J. Haantjes and G. J. Lubben, "Errors of Magnetic Deflection, II," *Philips Res. Rep.*, **14**, p. 65 (1959).
[3] J. Kaashoek, "A Study of Magnetic-Deflection Errors," *Philips Res. Rep.*, Suppl. **11**, p. 1 (1968).
[4] N. H. Dekkers, "A Universal Deflection Unit Generating a Field of Any Order and Azimuth," *J. Phys. D: Appl. Phys.*, **7**, p. 805 (1974).
[5] H. Ohiwa, "The Design of Deflection Coils," *J. Phys. D: Appl. Phys.*, **10**, p. 1437 (1977).
[6] D. E. Lobb, "Properties of Some Useful Two-Dimensional Magnetic Fields," *Nucl. Instrum. Methods*, **64**, p. 251 (1968).
[7] M. E. Carpenter, R. A. Momberger, and T. W. Shultz, "Application of Computer Modeling to Color Television Picture Tube Systems," *IEEE Trans. Consumer Electronics*, **CE-23**, p. 22 (1977).
[8] D. M. Fye, "An Integral Equation Method for the Analysis of Magnetic Deflection Yokes," *J. Appl. Phys.*, **50**, p. 17 (1979).
[9] Y. Yokota and T. Toyofuku, "The Calculation of the Deflection Magnetic Field and The Electron-Beam Trajectory for Color Television," *IEEE Trans. Consumer Electronics*, **CE-25**, p. 91 (1979).
[10] See, e.g., W. H. Hayt, *Engineering Electromagnetics*, 4th Ed., McGraw-Hill, N.Y. (1981), pp. 238–241.
[11] I. S. Gradshteyn and I. M. Ryzhik, *Table of Integrals, Series, and Products*, Academic Press, N.Y. (1980), pp. 389 and 1039–1045.
[12] See pp. 948–949 of Ref. [11].
[13] W. A. L. Heijnemans, M. A. M. Nieuwendijk, and N. G. Vink, "The Deflection Coils of the 30AX Color-Picture System," *Philips Tech. Rev.*, **39**, p. 154 (1980).
[14] B. B. Dasgupta, "Effect of Finite Coil Thickness in a Magnetic Deflection System," *J. Appl. Phys.*, **54**, p. 1626 (1983).

[15] J. Haantjes and G. J. Lubben, "Errors of Magnetic Deflection, I," *Philips Res. Rep.*, **12,** p. 46 (1957).
[16] F. J. Campbell, private communications.
[17] B. B. Dasgupta, "Theory of Large-Angle Deflection of Electrons in the Magnetic Field Inside a Television Tube," *RCA Rev.*, **43,** p. 548 (1982).
[18] B. B. Dasgupta, "Calculation of Inductance of the Horizontal Coil of a Magnetic-Deflection Yoke," *IEEE Trans. Consumer Electronics*, **CE-28,** p. 455 (1982).